New targets of urocortin-mediated cardioprotection

Seán P Barry[1], Kevin M Lawrence[4], James McCormick[1], Surinder M Soond[5], Mike Hubank[2], Simon Eaton[3], Ahila Sivarajah[6], Tiziano M Scarabelli[7], Richard A Knight[1], Christoph Thiemermann[6], David S Latchman[1], Paul A Townsend[8] and **Anastasis Stephanou[1]**

[1]Medical Molecular Biology Unit, [2]Department of Molecular Haematology and [3]Department of Surgery, Institute of Child Health, University College London, 30 Guilford Street, London, WC1N 1EH, UK

[4]Department of Cellular Pathology, St George's, University of London, Cranmer Terrace, Tooting, London, SW17 0RE, UK

[5]School of Biological Sciences, University of East Anglia, Norwich, NR4 7TJ, UK

[6]St Bartholomew's and The Royal London School of Medicine and Dentistry, William Harvey Research Institute, Centre for Translational Medicine and Therapeutics, Queen Mary University of London, London, EC1M 7BQ, UK

[7]Center for Heart and Vessel Preclinical Studies, St John Hospital and Medical Center, Wayne State University School of Medicine, 22201 Moross Road, Detroit, Michigan 48336, USA

[8]Human Genetics Division, MP808, Southampton General Hospital, University of Southampton, Southampton SO16 6YD, UK

(Correspondence should be addressed to S P Barry; Email: s.barry@ich.ucl.ac.uk)

Abstract

The urocortin (UCN) hormones UCN1 and UCN2 have been shown previously to confer significant protection against myocardial ischaemia/reperfusion (I/R) injury; however, the molecular mechanisms underlying their action are poorly understood. To further define the transcriptional effect of UCNs that underpins their cardioprotective activity, a microarray analysis was carried out using an *in vivo* rat coronary occlusion model of I/R injury. Infusion of UCN1 or UCN2 before the onset of reperfusion resulted in the differential regulation of 66 and 141 genes respectively, the majority of which have not been described previously. Functional analysis demonstrated that UCN-regulated genes are involved in a wide range of biological responses, including cell death (e.g. X-linked inhibitor of apoptosis protein), oxidative stress (e.g. nuclear factor erythroid derived 2-related factor 1/nuclear factor erythroid derived 2-like 1) and metabolism (e.g. *Prkaa2/AMPK*). In addition, both UCN1 and UCN2 were found to modulate the expression of a host of genes involved in G-protein-coupled receptor (GPCR) signalling including *Rac2*, *Gnb1*, *Dab2ip* (*AIP1*), *Ralgds*, *Rnd3*, *Rap1a* and *PKA*, thereby revealing previously unrecognised signalling intermediates downstream of CRH receptors. Moreover, several of these GPCR-related genes have been shown previously to be involved in mitogen-activated protein kinase (MAPK) activation, suggesting a link between CRH receptors and induction of MAPKs. In addition, we have shown that both UCN1 and UCN2 significantly reduce free radical damage following myocardial infarction, and comparison of the UCN gene signatures with that of the anti-oxidant tempol revealed a significant overlap. These data uncover novel gene expression changes induced by UCNs, which will serve as a platform to further understand their mechanism of action in normal physiology and cardioprotection.

Journal of Molecular Endocrinology (2010) **45,** 69–85

Introduction

The urocortins (UCNs) are 40-amino acid homologues of the hypothalamic stress peptide corticotropin-releasing hormone (CRH), and are widely expressed in the heart, central nervous system, gut, skeletal muscle, skin and immune system (Davidson *et al.* 2009). There are three members: UCN1, UCN2 (also known as stresscopin-related peptide) and UCN3 (also known as stresscopin). UCNs exert their effects by binding to two classes of G-protein-coupled receptors (GPCRs), the corticotropin-releasing hormone receptors, CRHR1 and CRHR2, both of which can be expressed as multiple splice variants (Hillhouse *et al.* 2002). UCN1 interacts with both CRHR1 and CRHR2, although with a higher affinity for the latter, whereas UCN2 and UCN3 only bind to CRHR2. In the brain, the UCNs appear to counteract the stress-provoked anxiety produced by hypothalamic CRH, and are appetite suppressors (De Kloet 2003). In addition, they modulate glucose homoeostasis and metabolic activity in peripheral tissues (Kuperman & Chen 2008), while in the gut, they delay gastric emptying and promote colonic motility (Martinez *et al.* 2004). The UCNs have also been implicated in immune modulation (Baigent 2001).

UCNs have been shown to have beneficial effects on the cardiovascular system, which include protection against heart failure and ischaemia/reperfusion (I/R) injury (Scarabelli *et al.* 2002, Rademaker *et al.* 2007). UCN1 has varied cardiovascular effects, which include elevation of corticotrophin and cortisol levels,

DOI: 10.1677/JME-09-0148
0952–5041/10/045–069
Online version via http://www.endocrinology-journals.org

vasodilatation, promotion of increased blood flow, and elevation of heart rate, and positive chronotropic and ionotropic effects (Parkes *et al.* 1997). Cardiac expression of UCN1 is increased during hypoxia and hypertrophy, and circulating UCN1 levels are elevated in patients suffering from heart failure (Ng *et al.* 2004). Moreover, UCN1 administration has beneficial effects in experimental heart failure, including promotion of increased cardiac output, reduced peripheral resistance and decreased circulating levels of the vasoconstricting hormones such as angiotensin II, vasopressin and endothelin-1 (Rademaker *et al.* 2002, Scarabelli *et al.* 2002). UCN1 also lowered mean arterial pressure and circulating levels of atrial natriuretic peptide (ANP) and B-type natriuretic peptide (BNP), and continuous infusion significantly delayed the onset of experimental heart failure (Rademaker *et al.* 2005, 2007). UCN2 increased contractility in rabbit ventricular myocytes, and reduced diastolic pressure, increased left ventricular ejection fraction and increased cardiac output in a mouse heart failure model, effects which were lost in CRHR1-deficient mice (Bale *et al.* 2004, Yang *et al.* 2006).

Our group has previously demonstrated the protective effects of UCNs in I/R injury. UCN1 was shown to protect cultured cardiac myocytes from simulated I/R injury *in vitro* and reduce infarct size, protect against loss of mitochondrial permeability and enhance cardiac function in an *ex vivo* Langendorff model (Brar *et al.* 2000, Scarabelli *et al.* 2002, Townsend *et al.* 2007). UCN1 also reduced creatine phosphokinase release, decreased the numbers of cleaved caspase-3-positive cells and helped maintain the reserves of high energy phosphates during I/R injury (Scarabelli *et al.* 2002). The administration of UCN1 during experimental I/R *in vivo* reduces infarct size, lowers mean arterial pressure and reduces incidences of ventricular tachycardia and fibrillation (Schulman *et al.* 2002, Liu *et al.* 2005). Importantly, UCN1 can protect the heart when administered just prior to reperfusion, making it attractive as a possible therapeutic (Schulman *et al.* 2002). UCN2 has also been shown to protect cardiac myocytes from I/R injury *in vitro* and decrease infarct size in Langendorff perfused rat hearts exposed to I/R injury (Chanalaris *et al.* 2003, Brar *et al.* 2004). In agreement with a protective role for UCNs in the myocardium, deletion of the UCN receptor CRHR2 leads to increased susceptibility to I/R injury (Brar *et al.* 2004). Treatment of cardiac myocytes with UCNs induces the activity of the MEK1/2–ERK1/2 and phosphatidylinositol 3-kinase–AKT pathways, both of which appear to be necessary for full-fledged cardioprotection by these hormones (Brar *et al.* 2002, Chanalaris *et al.* 2003).

In order to identify the cardioprotective mechanisms of UCN1, we have used limited microarray analysis previously to identify the molecular pathways activated by UCN1. For example, we have shown that UCN1 increases the expression of the Kir 6.1 cardiac potassium channel subunit in the Langendorff perfused rat heart, and the cardioprotective effects of UCN1 are inhibited by selective Kir 6.1 channel blockers (Lawrence *et al.* 2002). In similar studies, we have also shown that UCN1 increases the expression and activation of protein kinase Cε (PKCε; Lawrence *et al.* 2005), but attenuates the expression of calcium-insensitive phospholipase A2 (Lawrence *et al.* 2003).

It is currently unknown whether UCN1 and UCN2 mediate their cardioprotective effects through similar or distinct mechanisms. Although they are both equally cardioprotective, UCN2 binds exclusively to CRHR2 and thus may induce a separate cardioprotective programme towards UCN1. To address this question and to identify new possible targets of UCN-dependent cardioprotection, we have performed a microarray analysis to compare global gene expression profiles mediated by both UCN1 and UCN2 during I/R injury. In addition, we examined the effect of UCN treatment on I/R-induced oxidative stress. We have shown that UCN1 and UCN2 are as effective as the reactive oxygen species (ROS) scavenger tempol at lowering free radical damage during I/R injury. The changes in transcriptional profiles induced by UCNs were therefore compared to that of tempol, and overlap in differential expression was shown, suggesting that the protective effects of UCNs may also, in part, involve reducing free radical damage.

Materials and methods

This study was performed in accordance with the United Kingdom Home Office Animals (Scientific Procedures) Act 1986. All reagents were obtained from Sigma–Aldrich, unless otherwise stated.

In vivo I/R injury in rats

Coronary artery occlusion and reperfusion were performed as described previously in anaesthetised rats (Sivarajah *et al.* 2005). Briefly, male Wistar rats (255–285 g) were anaesthetised with thiopentone sodium (Intraval 120 mg/kg i.p). Anaesthesia was maintained by supplementary injections of thiopentone sodium as required. The trachea was cannulated, and the rats were ventilated using a Harvard ventilator (inspiratory oxygen concentration: 30%; 70 strokes/min, tidal volume: 8–10 ml/kg). Body temperature was maintained at 37 ± 1 °C, and the right carotid artery was cannulated and connected to a pressure transducer (Senso-Nor 840, Senso-Nor, Horten, Norway). The right jugular vein was then cannulated for the administration of drugs. A parasternal thoracotomy was then performed using an electrosurgery device to cauterise the intercostal arteries before cutting through three ribs.

The chest was retracted, and pericardium was dissected from the heart. The left anterior descending (LAD) coronary artery was isolated, and a snare occluder was placed around the LAD coronary artery. The retractor was then removed, and the rats were allowed to stabilise for 15 min. The occluder was tightened at time 0. After 25 min of LAD occlusion, the occluder was released to allow reperfusion for 2 h. At the end of the reperfusion period, the LAD coronary artery was reoccluded, and 1 ml of Evans Blue dye (2% w/v) was injected into the rats via the jugular vein. Evans Blue dye stains the tissue through which it is able to circulate, so the non-perfused vascular (occluded) tissue remains uncoloured. Each rat was killed with an overdose of anaesthetic, and the heart was excised and thoroughly washed with PBS. The heart was then sectioned into slices of 3–4 mm, the right ventricle wall was removed, and the risk area (the non-perfused and, hence, non-stained myocardium) was separated from the non-ischaemic (blue) tissue and immediately snap-frozen in liquid nitrogen. In each treatment group, the drug was infused 5 min prior to the onset of reperfusion. The treatment groups were as follows: i) sham operation or LAD occlusion with infusion of ii) saline, iii) 15 μg/kg UCN1, iv) 15 μg/kg UCN2 and v) 100 mg/kg tempol, $n=3$ per group. These doses were chosen based on previous studies (McDonald *et al.* 1999, Patel *et al.* 2004).

Determination of tissue malondialdehyde concentration

Levels of malondialdehyde (MDA), a marker of lipid peroxidation, in heart tissue were measured by HPLC. Tissue was homogenised using an Ultra-Turrax homogeniser in 2 ml of 50 mM potassium phosphate buffer (pH 6·0) containing 0·5% (w/v) hexadecyltri-methylammonium bromide. Twenty-five microlitres of homogenate were incubated with 2 μl of 0·2% (w/v) butylated hydroxytoluene in ethanol and 375 μl of 1% (v/v) phosphoric acid, and then derivatised with 345 μl of 15 mM 2-thiobarbituric acid at 100 °C for 60 min. Two hundred microlitres of the derivatised solution were collected and mixed with 200 μl of methanol. After the addition of 15 μl of 1 M KH_2PO_4 and 4 μl of 2 M KOH/2·4 M $KHCO_3$, samples were centrifuged (18 000 ***g*** for 10 min at 4 °C). HPLC was performed on a Hypersil 5-μm ODS column at a flow rate of 1 ml/min isocratically with an eluent of 65% 50 mM KH_2PO_4 (pH 7·0)/35% methanol. Fluorescence was monitored using a Jasco FP-1520 detector (excitation wavelength 515 nm and emission wavelength 553 nm), and the values of molar concentration were calculated by comparison with the reference solutions of derivatised MDA-tetrabutylammonium salt and were analysed in parallel. The concentration of MDA was expressed as μmol/g protein.

Affymetrix microarray analysis

RNA was extracted from the risk area of the left ventricle using TRIzol (Invitrogen). Biotinylated cRNA targets were prepared using the Ambion Message Amp II protocol: 15 μg of fragmented cRNA probes were added to 50 pM of control oligonucleotides (*bioB*, *bioC*, *bioD* and *Cre*), 30 μg of herring sperm DNA, 150 μg of BSA, 30 μl of DMSO and 150 μl of hybridisation buffer to a final volume of 300 μl, and heated to 99 °C for 5 min and then to 45 °C for 5 min. Two hundred microlitres of hybridisation mix were added to pre-hybridised Affymetrix rat expression 230A microarrays and rotated overnight at 60 r.p.m. for 16 h at 45 °C. Arrays were stained and washed on an Affymetrix GeneChip Fluidics Station 450 using the standard Affymetrix EukGE-WS2v4 script, and were scanned using an Affymetrix GeneChip scanner. Scanned images were obtained using Affymetrix GeneChip Operating Software, and all 15 microarrays passed quality control standards which included present calls $\geq 40\%$, scaling factor <2, GAPDH $3'/5'$ ratios <3 and RNA degradation plots, which showed equivalent slopes between microarrays. Downstream analysis was conducted using the Bioconductor R 2.8 programmes AffylmGUI (Wettenhall *et al.* 2006) and OneChannelGUI (Sanges *et al.* 2007). Background correction, normalisation and summarisation of the probe- level data into probe-set expression values were carried out using GC-Robust multi-array analysis from imported Affymetrix image (.CEL) files. Differential expression was calculated based on the Linear Models for Microarray (limma) statistics package in Bioconductor R, and multiple testing was corrected for using the Benjamini and Hochberg false discovery rate (FDR; Reiner *et al.* 2003). Genes were considered to be differentially expressed where there was a fold change ≥ 2 with an FDR-adjusted P value $\leq 0{\cdot}05$. Each transcript was annotated based on the gene identifiers present in the Affymetrix NetAffx database. Microarray data have been deposited at the EMBL-EBI ArrayExpress repository (http://www.ebi.ac. uk/micro-array-as/ae/, accession number E-MEXP-2098). Venn diagrams were constructed in Bioconductor R, and overlapping gene signatures between each treatment group were produced.

Ingenuity pathway analysis

To uncover functional groupings and putative interaction networks, lists of differentially expressed genes were analysed using Ingenuity Pathway Analysis (IPA) software (Ingenuity Systems, Redwood City, CA, USA). Datasets containing gene identifiers and expression values were mapped to the corresponding identifier in the Ingenuity Pathway Knowledge Base,

which ascribes functional groupings and known interactions from the published literature. This allows the identification of biological networks and functional pathways contained within each dataset. Fischer's test is used to calculate a *P* value, which determines whether the biological function assigned to the gene signature is due to chance alone. The IPA algorithm applies a score to rank networks based on the number of focus genes and the network size. Networks are related graphically where each gene is represented as a node; links between nodes denote biological relationships between genes and are supported by at least one peer-reviewed publication. Colour intensity signifies the levels of differential regulation and uncoloured nodes are integrated by the IPA algorithm, with them being relevant to the network but not differentially regulated in the input gene signature.

Quantitative real-time PCR

One microgram of RNA was extracted from the left ventricles of each of the treatment groups ($n=3$) or from neonatal myocytes ($n=3$ per group), and cDNA was prepared using Superscript II (Invitrogen). Quantitative PCR (qPCR) was carried out using Platinum SYBR Green (Invitrogen) on the DNA Engine Opticon system (MJ Research, Waltham, MA, USA). For PCRs, 5 μl of SYBR Green were added to 5 μl of cDNA with 500 nM primers in a 20-μl reaction mixture, and the PCR conditions were as follows: 95 °C for 3 min, followed by 40 cycles of 95 °C for 30 s, 60 °C for 30 s and 72 °C for 30 s. A melting curve analysis was performed from 65 to 95 °C by reading every 0·3 °C with a 1-s hold between reads. Specific primers were designed with the aid of CloneWorks and the Ensembl database, and are listed in Table 1. Wherever possible, primers were subjected to intron spanning, and for single-exon genes, a control cDNA reaction without reverse transcriptase was included to confirm the absence of genomic DNA, and all PCR products were visualised on agarose gels to ensure the presence of a single product. For each experiment, *Hprt*, β-actin and β2-microglobulin were used together as the normalising genes. PCR efficiency of both target and normalising genes was determined initially to ensure that the normalising genes were acceptable; to test primer efficiency, qPCR was carried out on a twofold dilution series from a pooled set of cDNAs, and the threshold C_t value was plotted against the log cDNA dilution. Efficiency was then calculated using the equation $m=(-1/\log E)$, where m is the slope of the line and E is the efficiency, and primer pairs were used only if the PCR efficiency of the normalising and control genes was found to be within 10% of each other (Schmittgen & Livak 2008). Expression changes were calculated using the $2^{-\Delta\Delta C_t}$ method, and expressed as fold change over control (Livak & Schmittgen 2001).

Western blot

Cardiac tissue from the risk area was snap-frozen in liquid nitrogen and ground to a fine powder using a pestle and mortar. The tissue was lysed in RIPA buffer (0·75 M NaCl, 5% (v/v) NP40, 2·5% (w/v) deoxycholate, 0·5% (w/v) SDS, 0·25 M Tris–HCl, pH 8·0, and 10 mM dithiothreitol- containing protease inhibitor

Table 1 Primer sequences used for quantitative PCR analysis

Genes	Forward	Reverse	Accession numbers
c-fos (Fos)	GCCTTTCCTACTACCATTCC	CCGTTTCTCTTCCTCTTCAG	NM_022197
Il1b	TTCAGGCAGGCAGTATCACT	CAGCATCTCGACAAGAGCTT	NM_031512
inos (Nos2)	AGCGGCTCCATGACTCTCA	TGCACCCAAACACCAAGGT	NM_012611
Mmp8	ATCTGGAGTGTGCCATCAAC	GCTGGGTTCTCTGTAAGCAT	NM_022221
Mmp9	GAAGACGACATAAAAGGCATCC	TCAGAAGGACCAGCAGTAG	NM_031055
Il6	ACTGCCTTCCCTACTTCACA	GCTCTGAATGACTCTGGCTT	NM_012589
Socs3	TGGTCACCCACAGCAAGTTT	ACCAGCTTGAGTACACAGTC	NM_053565.1
Dusp1	TACAGGAAGGACAGGATCTC	AGTGCACAAACACCCTTCCT	NM_053769
Icos	CGGTGTCCATCAAGAATCCA	ACGGGTAACCAAAGCTTCAG	NM_022610
Map4k2	CCGCTTGTGGATATGTATGG	ATTGTAGCCACCCTTGCGTT	NM_001106329
Bnip3	GTTCCAGCTTCCGTCTCTAT	CGCTTGTGTTTCTCATGCTG	NM_053420
Prkaa2	GGAATATGTGTCTGGAGGTG	GATCCACAGCTAGTTCGTAG	NM_023991.1
Xiap	GAGGGCTCACGGATTGGAA	ACTCACAAGATCTGCAATCAG	NM_022231.2
Hsp70	ACATGAAGCACTGGCCCTT	AAGATGAGCACGTTGCGCT	NM_031971.2
Nfe2l1	AGAGCCCGAGCCATGAAGA	TCAGTCACGGTCCTGTAAATT	NM_001108293
Dut	TCTGGGTGCTATGGAAGAGT	AAGCCTCCTGAGCCTCTCTC	NM_053592
β2-microglobulin	GTCTTTCTGGTGCTTGTCTCA	GTGAGCCAGGATATAGAAAGA	NM_012512
Hprt	CTCATGGACTGATTATGGACAGGAC	GCAGGTCAGCAAAGAACTTATAGCC	NM_012583
β-actin	AGATGACCCAGATCATGTTTGAG	AGGTCCAGACGCAGGATG	NM_031144

cocktail), and was centrifuged at 13 000 ***g*** to pellet cell debris. Protein concentration in the supernatant was determined using the BCA protein assay kit (Pierce, Rockford, IL, USA). Twenty micrograms of protein in Laemmli buffer were electrophoresed on 10% polyacrylamide gels, transferred onto Hybond-C nitrocellulose membranes (Amersham Biosciences) and blocked for 30 min in 4% non-fat dry milk in TBS. The following primary antibodies were used: AMP-activated protein kinase (AMPK)-α2 (PRKAA2; Abcam, Cambridge, UK), nuclear factor erythroid derived 2-related factor 1 (NFE2L1, also known as NRF1; Santa Cruz Biotechnology, Santa Cruz, CA, USA), X-linked inhibitor of apoptosis protein (XIAP; Santa Cruz Biotechnology), inducible HSP70 (iHSP70; Stressgen, Ann Arbor, MI, USA) and GAPDH (Chemicon, Billerica, MA, USA). Secondary antibodies were obtained from DAKO (Glostrup, Denmark).

Neonatal rat ventricular cardiac myocyte culture

Neonatal rat ventricular cardiac myocytes were isolated from the hearts of 1–3-day-old Sprague–Dawley rats. Hearts were removed and placed in oxygenated ADS buffer (116 mM NaCl, 5·4 mM KCl, 20 mM HEPES, 0·8 mM NaH_2PO_4, 405·7 μM $MgSO_4$ and 5·5 mM glucose, pH 7·35). Heart tissue was digested in 10 ml oxygenated ADS buffer supplemented with 0·1% collagenase and 0·025% pancreatin for 15 min, and the liberated cells were pelleted at 300 ***g*** for 5 min and resuspended in FBS. This digestion procedure was repeated seven times, after which, the cells were plated at 37 °C for 1 h to allow the adherence of fibroblasts. Myocytes were plated at a density of $2{\cdot}5\times10^5$/ml in DMEM with 40 units/ml penicillin (Gibco), 40 μg/ml streptomycin and 15% FBS. Cells were allowed to attach to the plates overnight, and the medium was replaced with DMEM containing 1% FBS. For I/R experiments, cells were incubated for 4 h in ischaemic buffer (137 mM NaCl, 12 mM KCl, 0·49 mM $MgCl_2$, 0·9 mM $CaCl_2$, 4 mM HEPES, 20 mM sodium lactate and 10 mM deoxyglucose, pH 6·2) in a 37 °C hypoxic chamber with 5% CO_2 and 95% argon. Following hypoxia, the medium was replaced with DMEM containing 1% FBS, and the cells were reoxygenated in 5% CO_2 in a 37 °C incubator for 4 h. For experimental controls, cells were incubated for 4 h in a control buffer (137 mM NaCl, 3·8 mM KCl, 0·49 mM $MgCl_2$, 0·9 mM $CaCl_2$, 4 mM HEPES and 10 mM glucose, pH 7·4), and then in DMEM containing 1% FBS.

Statistical analysis

Statistical analysis was carried out using Student's *t*-test or a one-way ANOVA with Dunnett's post test; *P* values of $<0{\cdot}05$ were considered significant. Error bars represent mean ± S.E.M.

Results

Differential gene expression mediated by UCN1 and UCN2 infusion during I/R injury

Both UCN1 and UCN2 have been shown to confer cardioprotection against ischaemic damage; however, little is known regarding the gene expression changes mediated by UCNs during I/R injury. We therefore sought to better understand the transcriptional effects that may underscore the protective activity of UCN hormones during I/R injury through the use of a microarray analysis. Male rats were subjected to either sham operation or 25-min ischaemia followed by 2-h reperfusion with infusion of saline, UCN1 or UCN2 prior to the onset of reperfusion. RNA was extracted from the left ventricle, and the microarray analysis was conducted using Affymetrix RAE 203A arrays. Genes were considered to be differentially expressed if there was a fold change ≥2 between the groups with an adjusted FDR *P* value $<0{\cdot}05$. The number of differentially expressed genes in each group is shown in Table 2. In total, I/R was found to differentially regulate 1055 genes compared to the sham group. UCN1 and UCN2 were compared to the I/R group in order to assess the effect of the hormones on I/R-dependent gene expression. UCN1 and UCN2 treatment resulted in the differential expression of 66 and 141 genes respectively. Of these, over half were *de novo* changes in gene expression rather than simply a reversal of gene expression changes induced by I/R injury (Table 3). To validate the microarray results, the expression of

Table 2 Numbers of differentially regulated probe sets and annotated genes differentially regulated in each group

	Probe sets	Annotated genes	Upregulated	Downregulated
Treatment				
Sham versus saline	1055	798	502	553
UCN1 versus saline	65	43	38	27
UCN2 versus saline	141	89	104	37
Tempol versus saline	66	38	52	14

Table 3 Number of genes in each treatment group that are regulated by ischaemia/reperfusion

Treatment	Regulated by I/R	Not regulated by I/R
UCN1	34	31
UCN2	81	59
Tempol	47	19

several transcripts that were differentially expressed during I/R was also assessed by qPCR (Table 4). Linear regression analysis gave an R^2 coefficient of 0·93 between qPCR and microarray analysis fold changes, demonstrating good correlation between differential expression measured by microarray analysis and qPCR (Fig. 1).

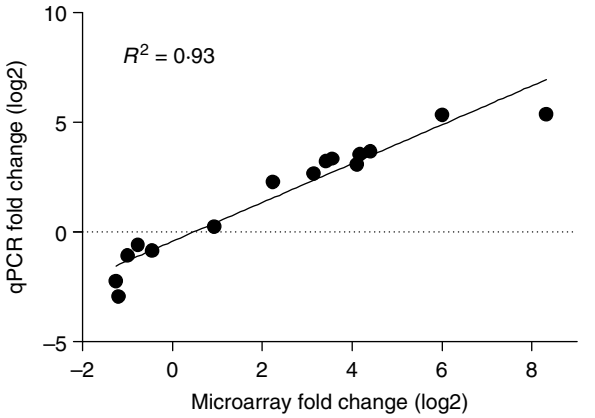

Figure 1 Validation of microarray analysis. Fold changes between the sham and I/R + saline groups obtained by microarray and qPCR were compared using linear regression.

IPA of UCN-mediated differential expression

The complete lists of annotated differentially expressed genes from the UCN1 and UCN2 treatment groups are presented in Tables 5 and 6. The majority of these gene expression changes are novel, and have not been reported previously as UCN-regulated gene expression changes; indeed, very few UCN2 downstream transcriptional targets have been documented previously. Of the 66 and 141 genes differentially regulated by UCN1 and UCN2, 30 were common to both peptides. This demonstrates that both UCNs induce distinct gene expression profiles during I/R injury; however, significant overlap exists between them.

IPA can uncover biological pathways and interaction networks between members in a list of differentially expressed genes. IPA identifies focus genes from the imported list, which it uses as a starting point to generate a biological network; *P* values for each network are assigned based on the number of focus genes in a given network compared to the presence of these genes in all networks in the IPA database. The highest ranking UCN1 network contained 15 focus genes, including cardioprotective genes such as *Xiap*, *Igf1*, *Syk*, *Cdh2* and nuclear factor erythroid derived 2-like 1 (*Nfe2l1*), as well as genes involved in G-protein signalling, including *Rac2*, *Gnb1* (transducin), *Prkaa2* (AMPK), *Prkar1a* (protein kinase A, PKA) and *Cap2* (Fig. 2). The highest ranking UCN2 network was more extensive, containing 25 focus genes from several classes. As with UCN1, there were several genes that participate in G-protein-related signalling including *Ras*, *Ralgds*, *Rnd3*, *Dab2IP* (AIP) and *Akap12*, as well as the apoptosis-associated genes *Eif2c*, *Tgm2*, *Mtif*, *Glrx2* and *Nfe2l1*, chaperones *Hspa4* (*Hsp70*) and *Dnaj13* (*Hsp40*) and the cytoskeletal genes *Rdx* and *Myo9b* (Fig. 2). The presence of several GPCR-related genes in the signalling networks prompted us to search for other differentially expressed genes involved in G-protein signalling, and in addition to the genes that have been mentioned already, UCN2 induced differential expression of *Rabgap1*, *Rap1a*, *Rhobt1*, *Cap2* and *Dnmbp*.

Both the UCN1 and UCN2 networks contained the mitogen-activated protein kinases (MAPKs) ERK and JNK as well as AKT as the central nodes, which anchored the networks. Although these kinases were not found to be transcriptionally regulated by either UCN hormone in this study, we have shown previously that both UCN1 and UCN2 can induce the phosphorylation and activation of MAPKs and AKT in cardiac myocytes (Brar *et al.* 2000, 2002, Chanalaris *et al.* 2003, 2005). Many of the G-protein-regulated genes that are induced by UCN1 and UCN2 lie upstream of MAPK activation; for example, *PKA*, *Rac2* and *Akap12* have been shown

Table 4 Comparison of fold changes obtained by microarray and qPCR

Genes	qPCR	Microarray
c-fos	64·1	40·8
Il1b	21·1	12·8
iNos	18	11·8
Mmp8	17·1	8·5
Mmp9	11·7	10·2
Il6	10·6	9·4
Socs3	8·8	6·4
Dusp1	4·7	4·9
Icos	1·9	1·2
Map4k2	−1·4	−1·8
Scn5a	−1·7	−1·5
Bnip3	−2	−2·1
Nfe2l1	−2·3	−7·6
Dut	−2·4	−4·7

Table 5 List of differentially expressed genes following urocortin 1 treatment during ischaemia/reperfusion injury

AffyID	Symbol	Gene title	Fold change	*P* value
1375788_at	*Rpl7*	Ribosomal protein L7	−10·3	0·00
1368894_at	*Cap2*	CAP, adenylate cyclase-associated protein, 2	7·0	0·04
1370745_at	*Slc34a1*	Solute carrier family 34 (sodium phosphate), member 1	−7·0	0·01
1369248_a_at	*Xiap*	X-linked inhibitor of apoptosis	4·8	0·03
1388246_at	*Clu*	Clusterin	−4·4	0·01
1370953_at	*Ccdc58*	Coiled-coil domain containing 58	−4·2	0·00
1375277_at	*Nrarp*	Notch-regulated ankyrin repeat protein	4·1	0·01
1373278_at	*Nfe2l1*	Nuclear factor erythroid derived 2-like 1	4·0	0·05
1375127_at	*Cox5a*	Cytochrome *c* oxidase, subunit Va	−3·8	0·03
1373229_at	*Lsm12*	LSM12 homologue (*S. cerevisiae*)	3·6	0·02
1367731_at	*Gnb1*	Guanine nucleotide-binding protein, beta 1	−3·3	0·00
1387865_at	*Dut*	Deoxyuridine triphosphatase	3·1	0·00
1368521_at	*Napsa*	Napsin A aspartic peptidase	−2·9	0·05
1370333_a_at	*Igf1*	Insulin-like growth factor 1	−2·8	0·03
1368946_at	*Arf2*	ADP-ribosylation factor 2	2·7	0·02
1373161_at	*Tmem98*	Transmembrane protein 98	2·6	0·03
1372404_at	*Rac2*	RAS-related C3 botulinum substrate 2	−2·6	0·02
1368911_at	*Kcnj8*	Potassium inwardly-rectifying channel, subfamily J, member 8	−2·5	0·04
1387259_at	*Cdh2*	Cadherin 2	2·4	0·05
1377060_at	*Mccc2*	Methylcrotonoyl-Coenzyme A carboxylase 2 (beta)	2·4	0·01
1387801_at	*Ppp6c*	Protein phosphatase 6, catalytic subunit	2·4	0·04
1387455_a_at	*Vldlr*	Very low density lipoprotein receptor	2·4	0·03
1375843_at	*Ids*	Iduronate 2-sulphatase	2·4	0·05
1399045_at	*Galnt1*	UDP-*N*-acetyl-alpha-D-galactosamine:polypeptide *N*-acetylgalactosaminyltransferase 1	2·4	0·01
1368186_a_at	*Syk*	Spleen tyrosine kinase	−2·4	0·03
1390478_at	*Orc4*	Origin recognition complex, subunit 4	2·3	0·05
1380547_at	*Clcn3*	Chloride channel 3	2·3	0·04
1389265_at	*Gbe1*	Glucan (1,4-alpha-), branching enzyme 1	2·3	0·02
1369654_at	*Prkaa2*	Protein kinase, AMP-activated, alpha 2 catalytic subunit	2·2	0·03
1373381_at	*Herc4*	Hect domain and RLD 4	2·2	0·02
1398795_at	*Dars*	Aspartyl-tRNA synthetase	2·2	0·03
1387872_at	*Hnrnpa1*	Heterogeneous nuclear ribonucleoprotein A1	2·2	0·02
1368235_at	*Clk3*	CDC-like kinase 3	−2·2	0·05
1373937_at	*Fyco1*	FYVE and coiled-coil domain containing 1	2·1	0·01
1388483_at	*Cfl2*	Cofilin 2, muscle	2·1	0·03
1388642_at	*Ei24*	Etoposide induced 2·4 mRNA	2·1	0·03
1386905_at	*Prkar1a*	Protein kinase, cAMP-dependent regulatory, type I, alpha	2·1	0·05
1387903_at	*Pja2*	Praja 2, RING-H2 motif containing	2·1	0·02
1389333_at	*Fbxo3*	F-box protein 3	2·1	0·03
1373472_at	*Actr6*	ARP6 actin-related protein 6 homologue	2·1	0·03
1374306_at	*Zdhhc18*	Zinc finger, DHHC domain containing 18	−2·1	0·02
1373152_at	*Prss23*	Protease, serine, 23	2·0	0·00
1377937_at	*Mrps14*	Mitochondrial ribosomal protein S14	2·0	0·03
1373069_at	*Mrps30*	Mitochondrial ribosomal protein S30	2·0	0·04

to activate ERK (Frost *et al.* 1996, Sun *et al.* 2007), while *Dab2ip* (*AIP1*), *Ralgds* and *Rnd3* are upstream of JNK (Zhang *et al.* 2004, Gonzalez-Garcia *et al.* 2005). This suggests that the identified biological networks may be centrally regulated at a post-translational level through UCN-mediated activation of intermediate kinases. This highlights the usefulness of network analysis for uncovering possible post-translational modification from a regulatory transcriptional network.

In order to ascertain whether the transcriptional network analysis held true at the protein level, we examined the expression of the members of the UCN1 network by western blot. We chose several proteins which may be important in the cardioprotective effects of UCNs (see Discussion). As a positive control, we first examined iHSP70 levels, which are known to be potently induced by I/R injury (Iwaki *et al.* 1993), and indeed in our model, we found that HSP70 could barely be detected in sham hearts, but that it was prominently upregulated by I/R (Fig. 3A). Unexpectedly, UCN2 appeared to increase protein expression (not seen at the mRNA level), and therefore, it may have unappreciated effects on HSP70 turnover. Both AMPK-α2/PRKAA2 and NFE2L1 (also known as NRF1) expression

Table 6 List of differentially expressed genes following urocortin 2 treatment during ischaemia/reperfusion injury

AffyID	Symbol	Gene title	Fold change	*P* value
1369718_at	*Ssr3*	Signal sequence receptor, gamma	6·3	0·02
1368894_at	*Cap2*	CAP, adenylate cyclase-associated protein, 2 (yeast)	5·2	0·05
1373278_at	*Nfe2l1*	Nuclear factor erythroid derived 2-like 1	5·2	0·03
1376175_at	*Gbas*	Glioblastoma amplified sequence	4·6	0·01
1368393_at	*C1qr1*	Complement component 1, q subcomponent, receptor 1	−4·1	0·05
1367534_at	*Rabgap1*	RAB GTPase-activating protein 1	−3·8	0·03
1390478_at	*Orc4*	Origin recognition complex, subunit 4	3·7	0·01
1370007_at	*Pdia4*	Protein disulphide isomerase-associated 4	3·7	0·01
1367825_at	*Ralgds*	Ral guanine nucleotide dissociation stimulator	−3·5	0·04
1388267_a_at	*Mt1a*	Metallothionein 1a	−3·4	0·03
1375788_at	*Rpl7*	Ribosomal protein L7	−3·3	0·02
1390728_at	*Limd1*	LIM domains containing 1	−3·3	0·02
1375138_at	*Timp3*	Tissue inhibitor of metalloproteinase 3	−3·3	0·03
1387865_at	*Dut*	Deoxyuridine triphosphatase	3·2	0·00
1375552_at	*Srp72*	Signal recognition particle 72	−3·2	0·02
1374640_at	*Them4*	Thioesterase superfamily member 4	3·1	0·03
1390125_at	*Tm9sf1*	Transmembrane 9 superfamily member 1	3·1	0·02
1368867_at	*Eif2c2*	Eukaryotic translation initiation factor 2C, 2	3·0	0·05
1386877_at	*Ap2s1*	Adaptor-related protein complex 2, sigma 1 subunit	3·0	0·03
1367562_at	*Sparc*	Secreted acidic cysteine-rich glycoprotein	−2·9	0·05
1372142_at	*Asna1*	arsA arsenite transporter, ATP-binding, homologue 1	2·9	0·02
1375542_at	*Rdx*	Radixin	2·9	0·02
1383065_at	*Nicn1*	Nicolin 1	2·9	0·03
1398914_at	*Polr2j*	Polymerase (RNA) II (DNA directed) polypeptide J	2·9	0·01
1389338_at	*Tmem126b*	Transmembrane protein 126B	2·9	0·03
1376066_at	*Rnd3*	Rho family GTPase 3	2·7	0·03
1374043_at	*Gramd3*	GRAM domain containing 3	2·7	0·02
1368182_at	*Acsl6*	Acyl-CoA synthetase long-chain family member 6	2·5	0·02
1377060_at	*Mccc2*	Methylcrotonoyl-Coenzyme A carboxylase 2 (beta)	2·5	0·01
1398795_at	*Dars*	Aspartyl-tRNA synthetase	2·5	0·01
1373472_at	*Actr6*	ARP6 actin-related protein 6 homologue	2·5	0·01
1373611_at	*Il17ra*	Interleukin 17 receptor A	−2·5	0·03
1375862_at	*Pxdn*	Peroxidasin homologue (*Drosophila*)	−2·5	0·02
1387617_at	*Tpm3*	Tropomyosin 3, gamma	−2·5	0·02
1370344_at	*Hspa4*	Heat shock protein 4	2·4	0·02
1389580_at	*Hltf*	Helicase-like transcription factor	2·4	0·03
1399073_at	*Otub1*	OTU domain, ubiquitin aldehyde binding 1	2·4	0·02
1372141_at	*Pfdn2*	Prefoldin 2	2·4	0·01
1373381_at	*Herc4*	Hect domain and RLD 4	2·4	0·01
1373161_at	*Tmem98*	Transmembrane protein 98	2·4	0·03
1375843_at	*Ids*	Iduronate 2-sulphatase	2·3	0·03
1387903_at	*Pja2*	Praja 2, RING-H2 motif containing	2·3	0·01
1389632_at	*Rhobtb1*	Rho-related BTB domain containing 1	2·3	0·02
1374695_at	*Cbx1*	Chromobox homologue 1 (*Drosophila* HP1 beta)	2·3	0·03
1387801_at	*Ppp6c*	Protein phosphatase 6, catalytic subunit	2·3	0·04
1375378_at	*Qk*	Quaking homologue, KH domain RNA binding	2·3	0·02
1375421_a_at	*Pja2*	Praja 2, RING-H2 motif containing	2·3	0·02
1368186_a_at	*Syk*	Spleen tyrosine kinase	−2·3	0·02
1368868_at	*Akap12*	A kinase (PRKA) anchor protein (gravin) 12	−2·3	0·04
1387866_at	*Myo9b*	Myosin Ixb	−2·3	0·02
1387455_a_at	*Vldlr*	Very low density lipoprotein receptor	2·2	0·03
1389265_at	*Gbe1*	Glucan (1,4-alpha-), branching enzyme 1	2·2	0·02
1373002_at	*Mrps9*	Mitochondrial ribosomal protein S9	2·2	0·02
1367609_at	*Mif*	Macrophage migration inhibitory factor	2·2	0·03
1398894_at	*Commd3*	COMM domain containing 3	2·2	0·02
1368470_at	*Ggh*	Gamma-glutamyl hydrolase	2·2	0·02
1373069_at	*Mrps30*	Mitochondrial ribosomal protein S30	2·2	0·02
1372189_at	*Dnajc13*	DnaJ (Hsp40) homologue, subfamily C, member 13	2·2	0·02
1372650_at	*Dnmbp*	Dynamin binding protein	2·2	0·05
1389534_at	*Ube2e3*	Ubiquitin-conjugating enzyme E2E 3, UBC4/5	2·2	0·02
1374518_at	*Tmem77*	Transmembrane protein 77	2·2	0·03

(continued)

Table 6 *Continued*

AffyID	Symbol	Gene title	Fold change	*P* value
1374183_at	*Eapp*	E2F-associated phosphoprotein	2·2	0·00
1370335_at	*Dab2ip*	Disabled homologue 2 (*Drosophila*) interacting protein	−2·2	0·05
1373757_at	*Trafd1*	TRAF type zinc finger domain containing 1	−2·2	0·05
1376319_at	*Sema3c*	Semaphorin 3C	2·2	0·04
1389327_at	*Mrpl32*	Mitochondrial ribosomal protein L32	2·1	0·05
1373186_at	*Slain2*	SLAIN motif family, member 2	2·1	0·00
1377262_at	Smek2	SMEK homologue 2, suppressor of mek1	2·1	0·01
1388882_at	*Fkbp3*	FK506-binding protein 3	2·1	0·02
1374318_at	*Brcc3*	BRCA1/BRCA2-containing complex, subunit 3	2·1	0·00
1388779_at	*Zfp180*	Zinc finger protein 180	2·1	0·04
1376690_at	*Med21*	Mediator complex subunit 21	2·1	0·01
1367628_at	*Lgals1*	Lectin, galactose binding, soluble 1	2·1	0·03
1389125_at	*Mrpl1*	Mitochondrial ribosomal protein L1	2·1	0·04
1389525_at	*Rnf149*	Ring finger protein 149	2·1	0·00
1368822_at	*Fstl1*	Follistatin-like 1	−2·1	0·05
1369943_at	*Tgm2*	Transglutaminase 2, C polypeptide	−2·1	0·02
1368338_at	*Cd52*	CD52 antigen	−2·1	0·03
1388615_at	*Rap1a*	RAS-related protein 1a	2·0	0·01
1389333_at	*Fbxo3*	F-box protein 3	2·0	0·03
1388780_at	*Terf2ip*	Telomeric repeat-binding factor 2, interacting protein	2·0	0·01
1390382_at	*Hypk*	Huntingtin interacting protein K	2·0	0·01
1373440_at	*Lyrm2*	LYR motif containing 2	2·0	0·00
1390259_at	*Ube2d1*	Ubiquitin-conjugating enzyme E2D 1, UBC4/5	2·0	0·04
1372865_at	*Zfp364*	Zinc finger protein 364	2·0	0·03
1367541_at	*Mettl5*	Methyltransferase like 5	2·0	0·03
1388803_at	*Dhps*	Deoxyhypusine synthase	2·0	0·03
1373675_at	*Glrx2*	Glutaredoxin 2 (thioltransferase)	2·0	0·01
1374472_at	*Vps37a*	Vacuolar protein sorting 37 homologue A	2·0	0·00
1370953_at	*Ccdc58*	Coiled-coil domain containing 58	−2·0	0·03

levels closely paralleled the microarray data, with decreased expression following I/R and restoration of protein levels by UCN1 and UCN2 (Fig. 3A); this was confirmed by densitometry (Fig. 3B). XIAP expression was dramatically reduced by I/R injury, and while microarray analysis did show a reduction in mRNA expression, it did not reach statistical significance. UCN1, but not UCN2, treatment led to increased mRNA expression of XIAP compared with I/R levels, and this was largely recapitulated at the protein level (Fig. 3A and B). These data suggest that the transcriptional network is indeed broadly representative of the true situation at the protein level, and also highlight potential novel regulators of UCN-mediated cardioprotection (see Discussion).

The regulation of AMPK-α2, NFE2L1 and XIAP during myocardial I/R injury has not been addressed previously, and since all three were downregulated in the whole heart by myocardial infarction, we were interested in examining their expression in cardiac myocytes. Thus to extend and confirm the *in vivo* findings, neonatal cardiac myocytes were subjected to simulated I/R injury. qPCR analysis revealed that the expression of all the three genes was reduced, thus confirming the regulation of these factors by I/R injury (Fig. 3C). As a control, increased expression of HSP70 following *in vitro* I/R injury is shown.

Molecular function analysis

In order to further classify the gene signatures for each hormone and place them in a functional context, molecular function analysis was carried out using IPA. The most significant functional groupings of genes regulated by UCN1 during I/R injury were those involved in cell death (e.g. *Xiap*, *Clu*, *Cdh2*, *Syk*, *Ei24*, *Gnb1* and *Nfe2l1*), cell growth (e.g. *IGF1*, *Vldlr*, *Rac2* and *Prkar1a*) and molecular transport (e.g. *Clcn3*, *Slc34a1* and *Prkaa2*); however, functional groupings encompassed a wide range of biological processes (Fig. 4A). From the UCN2 gene signature, the most significant functional groups were cell–cell signalling (e.g. *Cd93*, *Rdx*, *Rnd3*, *Tgm2*, *Timp3* and *Dnmbp*), cellular function and maintenance (e.g. *Cd93*, *Syk*, *Akap12* and *Asp21*), and cellular compromise (e.g. *Mt1f*, *Nfe2l1* and *Rdx*; Fig. 4B). This analysis demonstrates that the most significant molecular functions influenced by UCNs during I/R injury are those involved in controlling cell fate, and these genes may represent novel targets of UCNs in cardioprotection against I/R damage.

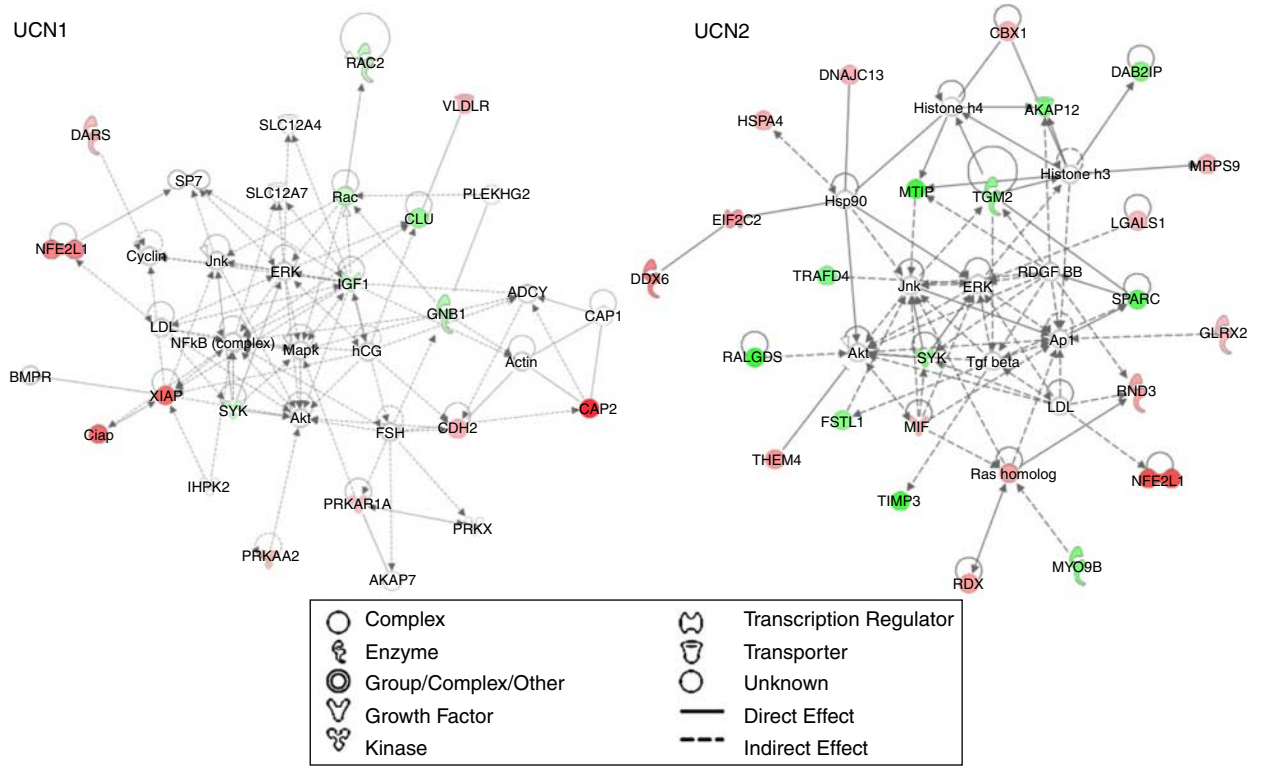

Figure 2 Ingenuity pathway analysis (IPA) of the UCN1 and UCN2 groups. Interactions are defined from the curated Ingenuity database, and comprise referenced published protein–protein interactions and transcriptional regulation. Upregulated genes are shown in red, and downregulated genes are shown in green; the intensity of the colour reflects the magnitude of the average fold changes. Solid lines represent direct gene–gene interactions, and broken lines represent indirect relationships, which may require genes not shown in the network. Uncoloured nodes are added by the IPA software, but are not present in the UCN1 or UCN2 gene list. Full colour version of this figure available via http://dx.doi.org/10.1677/JME-09-0148.

UCN1 and UCN2 inhibit free radical formation during I/R injury

Interestingly, both UCN1 and UCN2 gene expression signatures contained free radical scavenging as a functional group. Free radical damage plays a major role in the pathology of I/R injury, and inhibition of oxidative stress has been shown to significantly protect the myocardium from I/R-mediated cell death (McCormick *et al.* 2006). We therefore ascertained whether UCN1 and UCN2 were capable of suppressing I/R-dependent free radical formation. To this end, rats were subjected to ischaemia and were infused with saline, UCN1, UCN2 or the free radical scavenger tempol prior to the onset of reperfusion, and the level of lipid peroxidation was measured from left ventricular tissue using the MDA assay (Fig. 5A). As expected, I/R injury increased the MDA content in the left ventricles from $0{\cdot}46 \pm 0{\cdot}05$ to $0{\cdot}91 \pm 0{\cdot}08$ μmol/g. Remarkably, UCN1 and UCN2 lowered MDA levels to $0{\cdot}52 \pm 0{\cdot}13$ and $0{\cdot}38 \pm 0{\cdot}08$ μmol/g respectively, and this was compared with an MDA level of $0{\cdot}44 \pm 0{\cdot}03$ μmol/g in the tempol-treated group. Therefore, UCN1 and UCN2 treatment almost completely abolished the I/R-mediated increase in free radical levels, and indeed, UCN1 and UCN2 are as effective as tempol in reducing oxidative stress during I/R injury. Free radical inhibition may thus represent a major mechanism in the cardioprotective actions of the UCN hormones.

UCNs are unlikely to inhibit free radicals directly, rather the anti-oxidant activity is likely to be mediated through gene expression changes. To examine this possibility, the gene expression profiles of UCN1 and UCN2 were compared to that of tempol treatment during I/R injury. Tempol treatment resulted in the differential regulation of 66 genes (Table 2), and comparison with the UCN gene expression profiles revealed that 21/65 genes differentially regulated by UCN1 and 40/101 genes differentially regulated by UCN2 were also regulated by tempol (Fig. 5B). Therefore, ~30% of genes that were differentially regulated

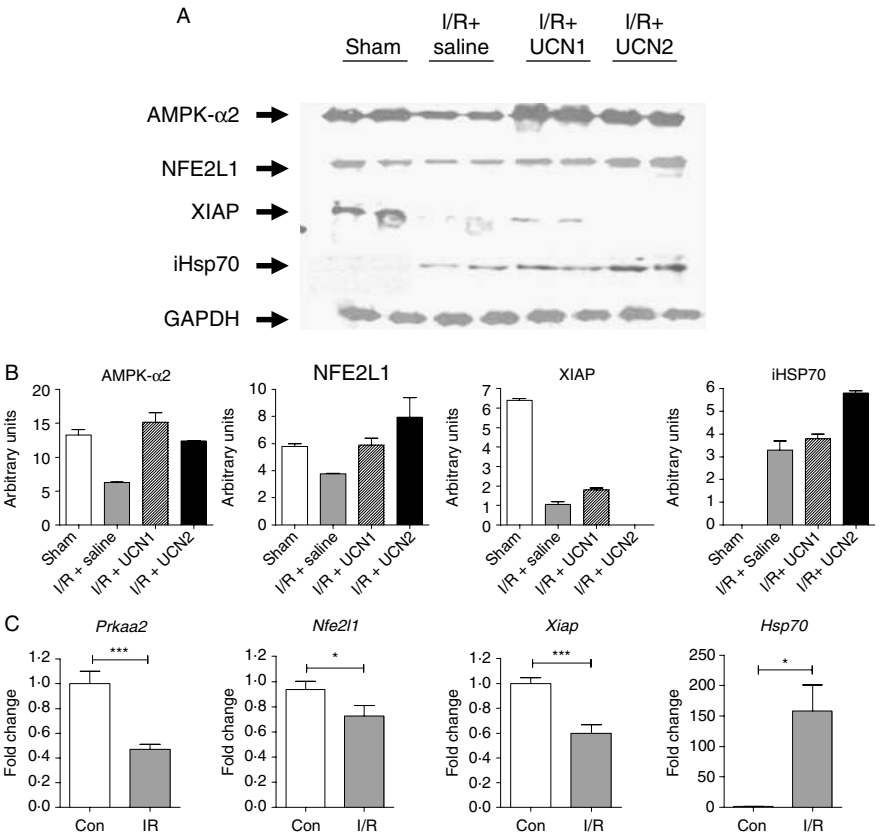

Figure 3 Regulation of AMPK, NFE2L1 and XIAP by I/R injury and urocortins. (A) The protein levels of AMPK-α2, NFE2L1, XIAP and iHSP70 were measured by western blot from each indicated group; GAPDH levels were used as a loading control. (B) Densitometry was carried out using Image J software and normalised to GAPDH levels; results are given as arbitrary units. (C) Neonatal rat ventricular myocytes were subjected to I/R injury, and the mRNA levels of the indicated genes were measured by qPCR. Statistical analysis was carried out using Student's *t*-test, $^{*}P<0{\cdot}05$, $^{***}P<0{\cdot}001$.

by UCN1 and UCN2 treatment during I/R injury were also regulated by anti-oxidant treatment. This suggests that a significant number of gene expression changes mediated by UCNs during I/R injury may be involved in the protection against oxidative stress in the myocardium.

There were a total of 18 annotated genes common to both UCN1 and UCN2, 15 of which were also differentially regulated by tempol (Fig. 5C). One of the most highly differentially regulated genes common to both was *Nfe2l1/Nrf1*, a member of the CNC (cap 'n' collar) basic leucine zipper family of transcription factors (Chen *et al.* 2003). *Nfe2l1* was upregulated 4·0-, 5·2- and 6·3-fold by UCN1, UCN2 and tempol respectively. NFE2L1 is a crucial mediator of oxidative stress, and is required for free radical scavenging and maintenance of redox potential (Kwong *et al.* 1999). It achieves this through binding to the anti-oxidant response element in a number of oxidative stress-regulated gene promoters (Ohtsuji *et al.* 2008). Of these 19 genes, *Nfe2l1* thus represents the most likely candidate common to both, which might be responsible for free radical inhibition and as such warrants further investigation.

Discussion

Both UCN1 and UCN2 have been shown to confer protection against myocardial infarction; however, their exact mechanism of action is poorly understood. Little is known particularly regarding how UCN2 affects the myocardium during I/R injury. Thus, a greater appreciation of downstream UCN signalling in the heart will greatly add to our understanding of both UCN biology and I/R injury. To address this, we carried out a microarray analysis on the hearts treated with UCN1 or UCN2. In our experimental model, UCNs were infused before the onset of reperfusion; the rationale for this approach is that any therapeutic

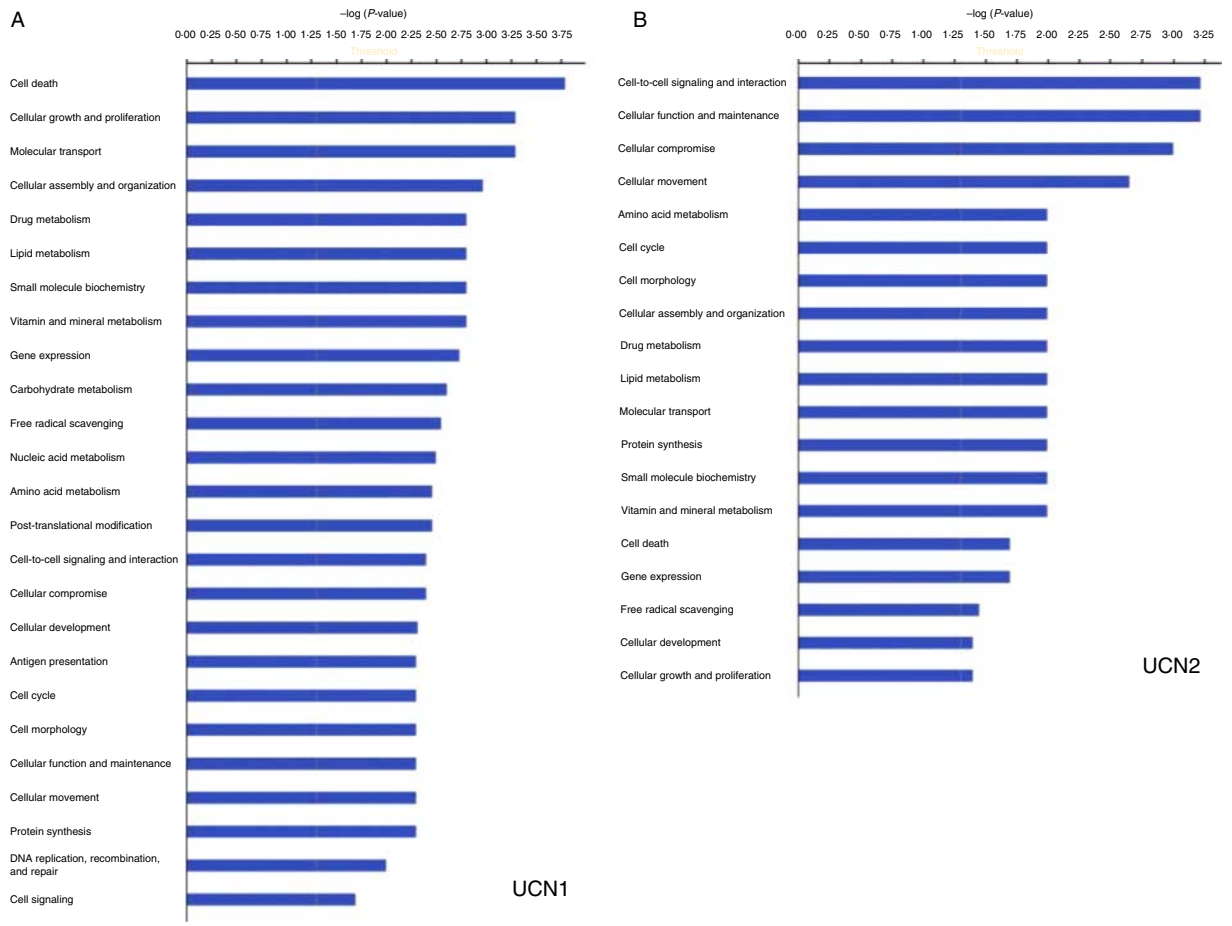

Figure 4 Ingenuity functional analysis of the UCN1 and UCN2 groups. Functional annotation of (A) the 66 probe sets in the UCN1 group and (B) the 141 probe sets in the UCN2 group identified as being differentially expressed when compared with saline infusion group during I/R. Groups are ranked according to the *P* value significance; the $P<0{\cdot}05$ threshold is shown. Full colour version of this figure available via http://dx.doi.org/10.1677/JME-09-0148.

intervention in a clinical setting would ideally be introduced before the surgical or medical induction of reperfusion to the ischaemic myocardium. Microarray analysis revealed a host of novel gene expression changes induced by both UCNs, which participate in a wide range of biological processes. Approximately, 50% of genes differentially regulated by UCN1 were also regulated by UCN2, showing significant overlapping functions. Since UCN2 signals only through CRHR2, the genes that are exclusive to UCN1 may represent a CRHR1-specific gene expression pattern. The possible role of UCN-mediated gene expression changes in the pathology of I/R injury will be discussed in turn.

GPCR-related genes

The UCN CRH receptors belong to the family of GPCRs, and binding to CRHR1 or CRHR2 stimulates G-protein and adenylyl cyclase activity; this in turn catalyses the conversion of ATP to cAMP, resulting in subsequent activation of PKA and PKC (Lawrence *et al.* 2005, Hillhouse & Grammatopoulos 2006, Kageyama *et al.* 2007). In addition, CRH phosphorylation by these kinases facilitates arrestin binding, leading to receptor desensitisation and uncoupling from G-proteins (Hillhouse & Grammatopoulos 2006). Several genes involved in GPCR and adenylyl cyclase signalling were found to be regulated by UCNs, including *Ralgds*, *Rhobtb1*, *Rnd3*, *Rap1a*, *Rabgap1*, *Prkaa2*, *Prkar1a*, *Cap2*, *Akap12*, *Gnb1*, *Dab2ip* and *Dnmbp*. The majority of these genes have not been shown previously to be regulated by UCNs or CRH receptors, and therefore, this reveals previously unknown signalling complexity following activation of CRH receptors. Since these G-protein-related genes were found to be both induced and repressed, UCNs may modulate the duration and strength of their signalling through altered expression of genes that are central to CRH receptor activity.

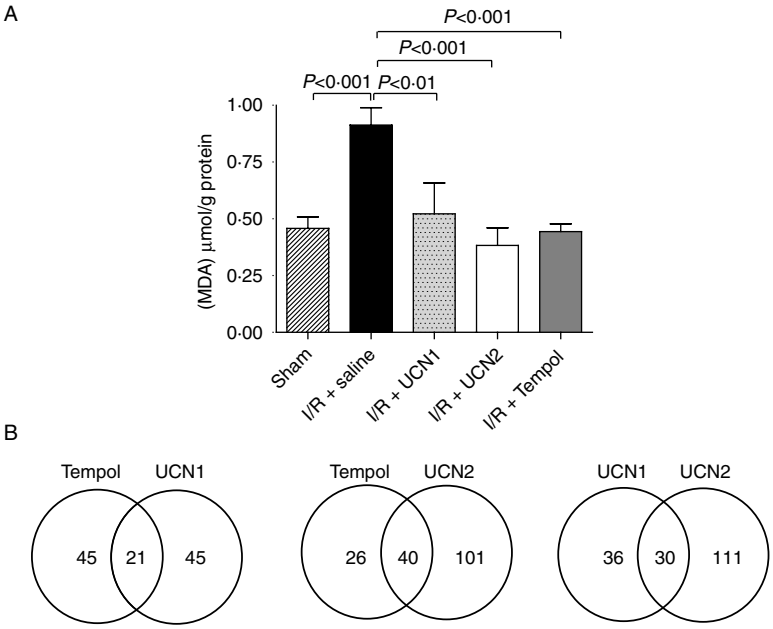

C

AffyID	Symbol	Gene title	UCN1	UCN2	Tempol
1375788_at	*Rpl7*	Ribosomal protein L7	–10·3	–3·3	–5·2
1368894_at	*Cap2*	CAP, adenylate cyclase-associated protein, 2	7·0	5·2	2·0
1370953_at	*Ccdc58*	Coiled-coil domain containing 58	–4·2	–2·1	–
1373278_at	*Nfe2l1*	Nuclear factor, erythroid derived 2,-like 1	4·0	5·2	6·3
1387865_at	*Dut*	Deoxyuridine triphosphatase	3·1	3·2	3·7
1373161_at	*Tmem98*	Transmembrane protein 98	2·6	2·4	2·4
1377060_at	*Mccc2*	Methylcrotonoyl-Coenzyme A carboxylase 2 (beta)	2·4	2·5	1·9
1387801_at	*Ppp6c*	Protein phosphatase 6, catalytic subunit	2·4	2·3	–
1387455_a_at	*Vldlr*	Very low density lipoprotein receptor	2·4	2·3	2·0
1375843_at	*Ids*	Iduronate 2-sulfatase	2·4	2·4	2·0
1373069_at	*Mrps30*	Mitochondrial ribosomal protein S30	2·0	2·2	1·8
1390478_at	*Orc4*	Origin recognition complex, subunit 4	2·3	3·7	3·2
1389265_at	*Gbe1*	Glucan (1,4-alpha-), branching enzyme1	2·3	2·2	2·1
1373381_at	*Herc4*	Hect domain and RLD 4	2·2	2·4	2·2
1398795_at	*Dars*	Aspartyl-tRNA synthetase	2·2	2·5	2·0
1387903_at	*Pja2*	Praja 2, RING-H2 motif containing	2·1	2·3	2·4
1389333_at	*Fbxo3*	F-box protein 3	2·1	2·0	–
1373472_at	*Actr6*	ARP6 actin-related protein 6 homolog	2·1	2·5	2·0

Figure 5 UCN1 and UCN2 inhibit free radical formation during I/R injury. (A) Saline, tempol, UCN1 and UCN2 were infused after 25-min ischaemia, followed by 2-h reperfusion ($n=5$ rats). The left ventricles were extracted, and tissue MDA levels were measured by HPLC. Error bars represent mean ± S.E.M. Statistical analysis was carried out using a one-way ANOVA with Dunnett's post test, $^{*}P<0{\cdot}05$, $^{***}P<0{\cdot}001$ compared with I/R + saline group. (B) Venn diagram depicting commonly expressed genes in each treatment group. (C) List of annotated genes that are differentially regulated by both UCN1 and UCN2. The level of differential expression between saline treatment and UCN1, UCN2 and tempol treatment is indicated.

Energy utilisation and metabolism

AMPK is activated by stresses which deplete cellular ATP levels such as those occurring during ischaemia, and is responsible for promoting fatty acid oxidation and increasing glucose uptake and glycolysis through the regulation of proteins such as GLUT4 (SLC2A4) and glycogen synthase (Dyck & Lopaschuk 2006). The mRNA and protein levels of AMPK-α2 (PRKAA2), which is the main cardiac isoform, were reduced following *in vivo* I/R injury, as were the mRNA levels in cardiac myocytes following *in vitro* I/R injury. UCN1 and UCN2 increased expression 2·3- and 1·9-fold respectively, and this was also confirmed at the protein

level, with UCN1 inducing slightly greater protein expression of AMPK-α2 than UCN2. AMPK activity was increased by PKA following GPCR stimulation, and interestingly, UCN1 also increased the expression of protein kinase, cAMP-dependent regulatory, type I, α (PRKAR1A), a regulatory subunit of PKA. UCN-mediated upregulation of AMPK is suggested to reduce ischaemic damage, since several reports have demonstrated that AMPK-α2 can protect the myocardium from I/R injury. Carvajal *et al.* (2007) found that AMPK-α2 deficiency resulted in reduced myocardial glucose uptake and glycogen content during I/R injury, leading to accelerated contracture. Mice expressing a kinase dead form of AMPK-α2 had exacerbated contractile dysfunction following I/R, accompanied by elevated TUNEL positivity and caspase-3 activity (Russell *et al.* 2004). AMPK has also been shown to avert hypoxic damage to cardiac myocytes by preventing endoplasmic reticulum stress (Terai *et al.* 2005). We have demonstrated previously improved myocardial energetics following UCN1 administration before reperfusion, and it is tempting to speculate that this energetic recovery of the ischaemic myocardium might be linked to increased AMPK levels (Scarabelli *et al.* 2002). In addition, AMPK has been shown to stimulate AKT activity in cardiac myocytes, and therefore, upregulation of AMPK expression may explain our previous observations of increased AKT activity in cardiac myocytes treated with UCN1 and UCN2 (Brar *et al.* 2002, Chanalaris *et al.* 2003, Bertrand *et al.* 2006).

Regulation of apoptosis

One of the most highly upregulated genes in the UCN1 group was *XIAP*, one of a family of six IAPs. XIAP functions by inhibiting the effector caspase-3, -7 and -9 through ubiquitin-mediated degradation (Eckelman *et al.* 2006). XIAP also protects from ROS-induced apoptosis through the promotion of increased expression of anti-oxidative genes (Resch *et al.* 2008). There are few studies addressing the role of XIAP in the myocardium; however, we have shown previously that the cardioprotective action of minocycline was associated with increased XIAP expression (Scarabelli *et al.* 2004). XIAP has also been shown to function as an anti-apoptotic factor in a stroke model of I/R injury (Zhu *et al.* 2007, Russell *et al.* 2008). We have found that XIAP levels are reduced following *in vivo* I/R injury, and that mRNA levels are reduced in cardiac myocytes following I/R injury *in vitro*. UCN1 administration partially restored XIAP expression, albeit not to the sham levels. We have shown previously that UCN1 treatment reduces the number of caspase-3-positive endothelial cells and cardiac myocytes following I/R injury *in vivo*, and it is therefore tempting to speculate that some of the anti-apoptotic effects of UCN1 may be mediated through reduced executioner caspase activity via XIAP upregulation (Scarabelli *et al.* 2002).

Genes involved in the regulation of oxidative stress

Both UCN1 and UCN2 significantly lowered MDA levels, showing that they inhibit free radical formation during I/R injury; indeed, they were as potent as the free radical scavenger tempol as anti-oxidants. Approximately 30% of genes regulated by UCN1 and UCN2 were also found to be regulated by tempol during I/R injury. These genes may comprise an anti-oxidant signature responsible for UCN-mediated free radical inhibition. Of the gene expression changes common to both hormones, one candidate which may account for the free radical inhibition was the anti-oxidant response gene *Nfe2l1* (*Nrf1*). *In vivo* I/R injury reduced the mRNA and protein levels of NFE2L1, while *Nfe2l1* mRNA levels were also reduced in cardiac myocytes following *in vitro* I/R injury. Both UCN1 and UCN2 significantly increased *Nfe2l1* expression (4·0- and 5·2-fold respectively), and the protein expression closely mirrored this, with UCN2 inducing greater NFE2L1 protein expression than UCN1. The physiological effect of reduced NFE2L1 levels during I/R is unknown, but some conclusions can be drawn from the studies of NFE2L1 deficiency. *Nfe2l1* knockout mice die at mid-gestation; however, analysis of NFE2L1-deficient foetal livers demonstrated exuberant oxidative stress due to insufficient expression of genes for the anti-oxidants GSH and GSSG, while NFE2L1-deficient fibroblasts displayed increased levels of cell death when treated with oxidants (Kwong *et al.* 1999, Chen *et al.* 2003). Taken together, these findings suggest that transcriptional repression of *Nfe2l1* leads to reduced levels of anti-oxidants during I/R injury, which may sensitise cardiac myocytes to oxidative stress. In this setting, upregulation of *Nfe2l1* levels by UCN1 and UCN2 may be important in aiding free radical scavenging and protection from I/R injury. However, it is unknown whether there is sufficient time within the 2-h reperfusion period for the increased levels of NFE2L1 protein to in turn upregulate oxidative response genes and account for the reduction in oxidative stress. More detailed kinetic analysis of the effect of UCNs on downstream NFE2L1 targets is needed to address this question.

It is not clear why UCN2 treatment led to a greater increase in *Nfe2l1* expression than UCN1 treatment; however, the *Nfe2l1* promoter contains binding sites for several transcriptional regulators including SP1, AP2, C/EBP and CBP (Luna *et al.* 1995), which may be regulated to different extents by UCN1 and UCN2. It must be noted that UCN1 and UCN2 did not increase *Nfe2l1* levels to the same extent as tempol (4·0-, 5·2- and

6·3-fold respectively); however, while NFE2L1 may indeed represent a major mediator of UCN-dependent free radical inhibition, additional genes are likely to be involved. Other candidates for the ROS- sparing effects of UCNs include glutaredoxin 2 (*Glrx2*), which was found to be reduced by 2·0-fold by I/R and increased by 1·6-fold by UCN1 treatment and by 2·0-fold by UCN2 treatment. GLRX2 catalyses the deglutathionylation of protein-glutathione mixed disulphides, and is involved in the maintenance of redox homoeostasis (Lillig *et al.* 2008). Transgenic overexpression of GLRX2 conferred protection against doxorubicin-mediated cardiac damage by increasing left ventricular function associated with increased levels of mitochondrial *S*-glutathionylation (Diotte *et al.* 2009). In addition, GLRX2 transgenic mice showed reduced infarct sizes and decreased ROS production following I/R injury, accompanied by reduced activity of caspase-3 and -9 (Nagy *et al.* 2008). These effects were dependent on AKT activity, suggesting that UCN1- and UCN2-mediated AKT activation in cardiac myocytes may lead to the restoration of GLRX2 levels following I/R injury, which in addition to enhanced *Nfe2l1* expression may contribute to the decrease in ROS production associated with UCN treatment. Reduction of *Rac2* expression caused by UCN1 may represent another potential candidate for reduced anti-oxidant activity. RAC2 GTPase is critical in the regulation of NADPH oxidase (NOX) function, and promotes NOX-dependent generation of superoxide anions (Diebold & Bokoch 2001). *Rac2* was upregulated 3·4-fold by I/R, and it was downregulated 2·6-fold by UCN1 but not by UCN2; reduced RAC2 levels in UCN1-treated animals may therefore reduce NOX activity and subsequent ROS production.

In conclusion, although many of the gene expression changes presented here remain to be corroborated by protein expression data, these findings nonetheless highlight previously unidentified effects of UCNs on the myocardium. We have identified a host of genes which may be intimately involved in signalling downstream of the CRH GPCRs. Many of the expression changes described may be central to the cardioprotective activity of UCN1 and UCN2; however, cardioprotection is more likely to be due to the combined effects of many transcriptional, post-transcriptional and translational changes acting in concert. Further characterisation of these newly identified putative UCN target genes not only will reveal new aspects to UCN biology, but may also uncover novel pharmacological targets for the treatment of I/R injury. Inhibition of free radical generation by both UCNs may be central to their cardioprotective activity, and the anti-oxidant response genes *Nfe2l1*, *Glrx2* and *Rac2* may have a role to play in this effect, and therefore, warrant further investigation.

Declaration of interest

The authors declare that there is no conflict of interest that could be perceived as prejudicing the impartiality of the research reported.

Funding

This study was funded by the British Heart Foundation. Grant number FS/03/111.

References

Baigent SM 2001 Peripheral corticotropin-releasing hormone and urocortin in the control of the immune response. *Peptides* **22** 809–820.

Bale TL, Hoshijima M, Gu Y, Dalton N, Anderson KR, Lee KF, Rivier J, Chien KR, Vale WW & Peterson KL 2004 The cardiovascular physiologic actions of urocortin II: acute effects in murine heart failure. *PNAS* **101** 3697–3702.

Bertrand L, Ginion A, Beauloye C, Hebert AD, Guigas B, Hue L & Vanoverschelde JL 2006 AMPK activation restores the stimulation of glucose uptake in an *in vitro* model of insulin-resistant cardiomyocytes via the activation of protein kinase B. *American Journal of Physiology. Heart and Circulatory Physiology* **291** H239–H250.

Brar BK, Jonassen AK, Stephanou A, Santilli G, Railson J, Knight RA, Yellon DM & Latchman DS 2000 Urocortin protects against ischemic and reperfusion injury via a MAPK-dependent pathway. *Journal of Biological Chemistry* **275** 8508–8514.

Brar BK, Stephanou A, Knight R & Latchman DS 2002 Activation of protein kinase B/Akt by urocortin is essential for its ability to protect cardiac cells against hypoxia/reoxygenation-induced cell death. *Journal of Molecular and Cellular Cardiology* **34** 483–492.

Brar BK, Jonassen AK, Egorina EM, Chen A, Negro A, Perrin MH, Mjos OD, Latchman DS, Lee KF & Vale W 2004 Urocortin-II and urocortin-III are cardioprotective against ischemia reperfusion injury: an essential endogenous cardioprotective role for corticotropin releasing factor receptor type 2 in the murine heart. *Endocrinology* **145** 24–35.

Carvajal K, Zarrinpashneh E, Szarszoi O, Joubert F, Athea Y, Mateo P, Gillet B, Vaulont S, Viollet B, Bigard X *et al.* 2007 Dual cardiac contractile effects of the α2-AMPK deletion in low-flow ischemia and reperfusion. *American Journal of Physiology. Heart and Circulatory Physiology* **292** H3136–H3147.

Chanalaris A, Lawrence KM, Stephanou A, Knight RD, Hsu SY, Hsueh AJ & Latchman DS 2003 Protective effects of the urocortin homologues stresscopin (SCP) and stresscopin-related peptide (SRP) against hypoxia/reoxygenation injury in rat neonatal cardiomyocytes. *Journal of Molecular and Cellular Cardiology* **35** 1295–1305.

Chanalaris A, Lawrence KM, Townsend PA, Davidson S, Jamshidi Y, Stephanou A, Knight RD, Hsu SY, Hsueh AJ & Latchman DS 2005 Hypertrophic effects of urocortin homologous peptides are mediated via activation of the Akt pathway. *Biochemical and Biophysical Research Communications* **328** 442–448.

Chen L, Kwong M, Lu R, Ginzinger D, Lee C, Leung L & Chan JY 2003 Nrf1 is critical for redox balance and survival of liver cells during development. *Molecular and Cellular Biology* **23** 4673–4686.

Davidson SM, Rybka AE & Townsend PA 2009 The powerful cardioprotective effects of urocortin and the corticotropin releasing hormone (CRH) family. *Biochemical Pharmacology* **77** 141–150.

De Kloet ER 2003 Hormones, brain and stress. *Endocrine Regulations* **37** 51–68.

Diebold BA & Bokoch GM 2001 Molecular basis for Rac2 regulation of phagocyte NADPH oxidase. *Nature Immunology* **2** 211–215.

Diotte NM, Xiong Y, Gao J, Chua BH & Ho YS 2009 Attenuation of doxorubicin-induced cardiac injury by mitochondrial glutaredoxin 2. *Biochimica et Biophysica Acta* **1793** 427–438.

Dyck JR & Lopaschuk GD 2006 AMPK alterations in cardiac physiology and pathology: enemy or ally? *Journal of Physiology* **574** 95–112.

Eckelman BP, Salvesen GS & Scott FL 2006 Human inhibitor of apoptosis proteins: why XIAP is the black sheep of the family. *EMBO Reports* **7** 988–994.

Frost JA, Xu S, Hutchison MR, Marcus S & Cobb MH 1996 Actions of Rho family small G proteins and p21-activated protein kinases on mitogen-activated protein kinase family members. *Molecular and Cellular Biology* **16** 3707–3713.

Gonzalez-Garcia A, Pritchard CA, Paterson HF, Mavria G, Stamp G & Marshall CJ 2005 RalGDS is required for tumor formation in a model of skin carcinogenesis. *Cancer Cell* **7** 219–226.

Hillhouse EW & Grammatopoulos DK 2006 The molecular mechanisms underlying the regulation of the biological activity of corticotropin-releasing hormone receptors: implications for physiology and pathophysiology. *Endocrine Reviews* **27** 260–286.

Hillhouse EW, Randeva H, Ladds G & Grammatopoulos D 2002 Corticotropin-releasing hormone receptors. *Biochemical Society Transactions* **30** 428–432.

Iwaki K, Chi SH, Dillmann WH & Mestril R 1993 Induction of HSP70 in cultured rat neonatal cardiomyocytes by hypoxia and metabolic stress. *Circulation* **87** 2023–2032.

Kageyama K, Hanada K, Moriyama T, Imaizumi T, Satoh K & Suda T 2007 Differential regulation of CREB and ERK phosphorylation through corticotropin-releasing factor receptors type 1 and 2 in AtT-20 and A7r5 cells. *Molecular and Cellular Endocrinology* **263** 90–102.

Kuperman Y & Chen A 2008 Urocortins: emerging metabolic and energy homeostasis perspectives. *Trends in Endocrinology and Metabolism* **19** 122–129.

Kwong M, Kan YW & Chan JY 1999 The CNC basic leucine zipper factor, Nrf1, is essential for cell survival in response to oxidative stress-inducing agents. Role for Nrf1 in gamma-gcs(l) and gss expression in mouse fibroblasts. *Journal of Biological Chemistry* **274** 37491–37498.

Lawrence KM, Chanalaris A, Scarabelli T, Hubank M, Pasini E, Townsend PA, Comini L, Ferrari R, Tinker A, Stephanou A *et al.* 2002 K(ATP) channel gene expression is induced by urocortin and mediates its cardioprotective effect. *Circulation* **106** 1556–1562.

Lawrence KM, Scarabelli TM, Turtle L, Chanalaris A, Townsend PA, Carroll CJ, Hubank M, Stephanou A, Knight RA & Latchman DS 2003 Urocortin protects cardiac myocytes from ischemia/reperfusion injury by attenuating calcium-insensitive phospholipase A2 gene expression. *FASEB Journal* **17** 2313–2315.

Lawrence KM, Kabir AM, Bellahcene M, Davidson S, Cao XB, McCormick J, Mesquita RA, Carroll CJ, Chanalaris A, Townsend PA *et al.* 2005 Cardioprotection mediated by urocortin is dependent on PKCepsilon activation. *FASEB Journal* **19** 831–833.

Lillig CH, Berndt C & Holmgren A 2008 Glutaredoxin systems. *Biochimica et Biophysica Acta* **1780** 1304–1317.

Liu CN, Yang C, Liu XY & Li S 2005 *In vivo* protective effects of urocortin on ischemia–reperfusion injury in rat heart via free radical mechanisms. *Canadian Journal of Physiology and Pharmacology* **83** 459–465.

Livak KJ & Schmittgen TD 2001 Analysis of relative gene expression data using real-time quantitative PCR and the 2(−Delta Delta C(T)) method. *Methods* **25** 402–408.

Luna L, Skammelsrud N, Johnsen O, Abel KJ, Weber BL, Prydz H & Kolsto AB 1995 Structural organization and mapping of the human TCF11 gene. *Genomics* **27** 237–244.

Martinez V, Wang L, Million M, Rivier J & Tache Y 2004 Urocortins and the regulation of gastrointestinal motor function and visceral pain. *Peptides* **25** 1733–1744.

McCormick J, Barry SP, Sivarajah A, Stefanutti G, Townsend PA, Lawrence KM, Eaton S, Knight RA, Thiemermann C, Latchman DS *et al.* 2006 Free radical scavenging inhibits STAT phosphorylation following *in vivo* ischemia/reperfusion injury. *FASEB Journal* **20** 2115–2117.

McDonald MC, Zacharowski K, Bowes J, Cuzzocrea S & Thiemermann C 1999 Tempol reduces infarct size in rodent models of regional myocardial ischemia and reperfusion. *Free Radical Biology and Medicine* **27** 493–503.

Nagy N, Malik G, Tosaki A, Ho YS, Maulik N & Das DK 2008 Overexpression of glutaredoxin-2 reduces myocardial cell death by preventing both apoptosis and necrosis. *Journal of Molecular and Cellular Cardiology* **44** 252–260.

Ng LL, Loke IW, O'Brien RJ, Squire IB & Davies JE 2004 Plasma urocortin in human systolic heart failure. *Clinical Science* **106** 383–388.

Ohtsuji M, Katsuoka F, Kobayashi A, Aburatani H, Hayes JD & Yamamoto M 2008 Nrf1 and Nrf2 play distinct roles in activation of antioxidant response element-dependent genes. *Journal of Biological Chemistry* **283** 33554–33562.

Parkes DG, Vaughan J, Rivier J, Vale W & May CN 1997 Cardiac inotropic actions of urocortin in conscious sheep. *American Journal of Physiology* **272** H2115–H2122.

Patel NS, Collin M & Thiemermann C 2004 Urocortin does not reduce the renal injury and dysfunction caused by experimental ischaemia/reperfusion. *European Journal of Pharmacology* **496** 175–180.

Rademaker MT, Charles CJ, Espiner EA, Fisher S, Frampton CM, Kirkpatrick CM, Lainchbury JG, Nicholls MG, Richards AM & Vale WW 2002 Beneficial hemodynamic, endocrine, and renal effects of urocortin in experimental heart failure: comparison with normal sheep. *Journal of the American College of Cardiology* **40** 1495–1505.

Rademaker MT, Charles CJ, Espiner EA, Frampton CM, Lainchbury JG & Richards AM 2005 Four-day urocortin-I administration has sustained beneficial haemodynamic, hormonal, and renal effects in experimental heart failure. *European Heart Journal* **26** 2055–2062.

Rademaker MT, Charles CJ & Richards AM 2007 Urocortin 1 administration from onset of rapid left ventricular pacing represses progression to overt heart failure. *American Journal of Physiology. Heart and Circulatory Physiology* **293** H1536–H1544.

Reiner A, Yekutieli D & Benjamini Y 2003 Identifying differentially expressed genes using false discovery rate controlling procedures. *Bioinformatics* **19** 368–375.

Resch U, Schichl YM, Sattler S & de Martin R 2008 XIAP regulates intracellular ROS by enhancing antioxidant gene expression. *Biochemical and Biophysical Research Communications* **375** 156–161.

Russell RR III, Li J, Coven DL, Pypaert M, Zechner C, Palmeri M, Giordano FJ, Mu J, Birnbaum MJ & Young LH 2004 AMP-activated protein kinase mediates ischemic glucose uptake and prevents postischemic cardiac dysfunction, apoptosis, and injury. *Journal of Clinical Investigation* **114** 495–503.

Russell JC, Whiting H, Szuflita N & Hossain MA 2008 Nuclear translocation of X-linked inhibitor of apoptosis (XIAP) determines cell fate after hypoxia ischemia in neonatal brain. *Journal of Neurochemistry* **106** 1357–1370.

Sanges R, Cordero F & Calogero RA 2007 oneChannelGUI: a graphical interface to Bioconductor tools, designed for life scientists who are not familiar with R language. *Bioinformatics* **23** 3406–3408.

Scarabelli TM, Pasini E, Stephanou A, Comini L, Curello S, Raddino R, Ferrari R, Knight R & Latchman DS 2002 Urocortin promotes hemodynamic and bioenergetic recovery and improves cell survival in the isolated rat heart exposed to ischemia/reperfusion. *Journal of the American College of Cardiology* **40** 155–161.

Scarabelli TM, Stephanou A, Pasini E, Gitti G, Townsend P, Lawrence K, Chen-Scarabelli C, Saravolatz L, Latchman D, Knight R *et al.* 2004 Minocycline inhibits caspase activation and reactivation, increases

the ratio of XIAP to smac/DIABLO, and reduces the mitochondrial leakage of cytochrome *C* and smac/DIABLO. *Journal of the American College of Cardiology* **43** 865–874.

Schmittgen TD & Livak KJ 2008 Analyzing real-time PCR data by the comparative *C*(T) method. *Nature Protocols* **3** 1101–1108.

Schulman D, Latchman DS & Yellon DM 2002 Urocortin protects the heart from reperfusion injury via upregulation of p42/p44 MAPK signaling pathway. *American Journal of Physiology. Heart and Circulatory Physiology* **283** H1481–H1488.

Sivarajah A, McDonald MC & Thiemermann C 2005 The cardioprotective effects of preconditioning with endotoxin, but not ischemia, are abolished by a peroxisome proliferator-activated receptor-γ antagonist. *Journal of Pharmacology and Experimental Therapeutics* **313** 896–901.

Sun LL, Cheng C, Liu HO, Shen CC, Xiao F, Qin J, Yang JL & Shen AG 2007 Src suppressed C kinase substrate regulates the lipopolysac-charide-induced TNF-α biosynthesis in rat astrocytes. *Journal of Molecular Neuroscience* **32** 16–24.

Terai K, Hiramoto Y, Masaki M, Sugiyama S, Kuroda T, Hori M, Kawase I & Hirota H 2005 AMP-activated protein kinase protects cardiomyocytes against hypoxic injury through attenuation of endoplasmic reticulum stress. *Molecular and Cellular Biology* **25** 9554–9575.

Townsend PA, Davidson SM, Clarke SJ, Khaliulin I, Carroll CJ, Scarabelli TM, Knight RA, Stephanou A, Latchman DS & Halestrap AP 2007 Urocortin prevents mitochondrial permeability transition in response to reperfusion injury indirectly by reducing oxidative stress. *American Journal of Physiology. Heart and Circulatory Physiology* **293** H928–H938.

Wettenhall JM, Simpson KM, Satterley K & Smyth GK 2006 affylmGUI: a graphical user interface for linear modeling of single channel microarray data. *Bioinformatics* **22** 897–899.

Yang LZ, Kockskamper J, Heinzel FR, Hauber M, Walther S, Spiess J & Pieske B 2006 Urocortin II enhances contractility in rabbit ventricular myocytes via CRF(2) receptor-mediated stimulation of protein kinase A. *Cardiovascular Research* **69** 402–411.

Zhang H, Zhang R, Luo Y, D'Alessio A, Pober JS & Min W 2004 AIP1/DAB2IP, a novel member of the Ras-GAP family, transduces TRAF2-induced ASK1-JNK activation. *Journal of Biological Chemistry* **279** 44955–44965.

Zhu C, Xu F, Fukuda A, Wang X, Fukuda H, Korhonen L, Hagberg H, Lannering B, Nilsson M, Eriksson PS *et al.* 2007 X chromosome-linked inhibitor of apoptosis protein reduces oxidative stress after cerebral irradiation or hypoxia–ischemia through up-regulation of mitochondrial antioxidants. *European Journal of Neuroscience* **26** 3402–3410.

Received in final form 29 April 2010
Accepted 24 May 2010
Made available online as an Accepted Preprint 25 May 2010